Article

pubs.acs.org/Biomac

In Vitro Ligament–Bone Interface Regeneration Using a Trilineage Coculture System on a Hybrid Silk Scaffold

Pengfei He,[†] Kian Siang Ng,[†] Siew Lok Toh,[†,‡] and James Cho Hong Goh*[,†,§]

Departments of [†]Bioengineering, [‡]Mechanical Engineering, and [§]Orthopaedic Surgery, National University of Singapore, Singapore 117576

ABSTRACT: The ligament–bone interface is a complex structure that comprises ligament, fibrocartilage, and bone. We hypothesize that mesenchymal stem cells cocultured in between ligament and bone cells, on a hybrid silk scaffold with sections suitable for each cell type, would differentiate into fibrocartilage. The section of scaffold for osteoblast seeding was coated with hydroxyapatite. A trilineage coculture system (osteoblasts–BMSCs–fibroblasts) on a hybrid silk scaffold was established. RT-PCR results and immunohistochemistry results demonstrated that BMSCs cocultured between fibroblasts and osteoblasts had differentiated into the fibrocartilaginous lineage. The morphological change was also observed by SEM observation. A gradual transition from the uncalcified to the calcified region was formed in the cocultured BMSCs from the region that directly interacted with fibroblasts to the region that directly interacted with osteoblasts. The role of transforming growth factor β3 (TGF-β3) in this trilineage coculture model was also investigated by supplementing the coculture system with 10 ng/mL TGF-β3. The TGF-treated group showed similar results of fibrocartilaginous differentiation of BMSCs with coculture group without TGF-β3 supplement. However, no calcium deposition was found in the cocultured BMSCs in the TGF-treated group. This may indicate TGF-β3 delayed the mineralization process of chondrocytes.

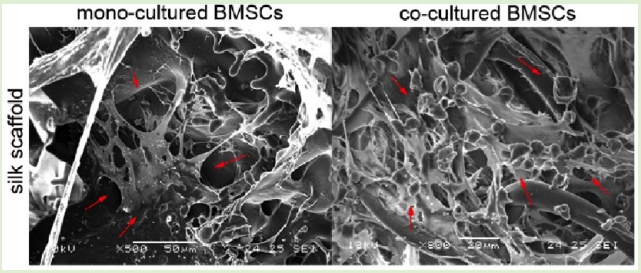

INTRODUCTION

It has been reported that about 100000 anterior cruciate ligament (ACL) reconstructions were performed annually in the United States.[1] The long-term performance of the graft used to replace the injured ACL mainly relies on the integration of the graft with the host bone.[2] Implanted ligament alone grafts are often lacking the ligament-to-bone interface, resulting in a poor ability of integration into the bone tissue and poor mechanical stability, which are the main reasons for graft failure.[3] The interface where the ligament merges with the bone is known as the enthesis. The enthesis is a multiphasic structure that comprises of three zones: ligament, fibrocartilage, and bone.[3,4] The fibrocartilage region can be further divided into uncalcified and calcified fibrocartilage zones. The calcified fibrocartilage zone is separated distinctly from uncalcified fibrocartilage zone by a tidemark, demarcating mineralized matrix. The fibrocartilage at the interface is the transitional zone of tissue to bridge the gap between the mechanical properties of ligament and bone.[5] The interface thus can facilitate the smooth transfer of force between soft and hard tissue when under mechanical loading.

Though the mechanism of the generation of enthesis is not clear, immunohistochemistry study of Gao et al. on the femoral attachment of the medial collateral ligament (MCL) of the rat knee joint provided some clues of the differentiation of fibrocartilage during entheses development.[6] In the fetus or newborn rat, the tendon/ligament initially attaches to the hyaline cartilage. Then the hyaline cartilage undergoes endochondral ossification and is replaced by bone. This hyaline cartilage was eventually completely resorbed and replaced by fibrocartilage developing in the ligament.[7,8] Thus, Lu and Jiang proposed a working hypothesis for interface regeneration, suggesting that heterotypic cellular interactions of osteoblast–fibroblast mediate interface regeneration, leading to phenotypic changes or *trans*-differentiation of osteoblasts and fibroblasts.[9] These interactions may also promote the differentiation of stem cells or progenitor cells into fibrochondrocytes, leading to the regeneration of the fibrocartilage interface. Based on this working hypothesis, Wang et al. established osteoblasts–fibroblasts coculture on a Petri dish using a hydrogel divider and found phenotypic changes and gene expression of interface-relevant markers in the 2D coculture.[10] Spalazzi and colleagues performed an in vivo study using triculture of fibroblasts, chondrocytes, and osteoblasts on a stratified PLGA scaffold and found fibrocartilage characteristic markers were exhibited in the chondrocyte-seeded phase between fibroblasts and osteoblasts.[11] On the other hand, the function of bone marrow mesenchymal stem cells (BMSCs) in the regeneration of interface was also investigated. Lim et al. coated tendon grafts with mesenchymal stem cells embedded in a fibrin gel.[12] They observed the formation of a cartilaginous tissue zone between graft and bone, which showed histologic characteristics similar to normal rabbit ACL insertions instead of scar tissues.

Received: April 26, 2012
Revised: July 13, 2012
Published: August 10, 2012

Their study suggested a potential role for stem cells in fibrocartilage formation at the interface.

Silk is a natural protein with appropriate biomechanical properties, good biocompatibility, and slow degradation rate. It is, therefore, a suitable scaffold for ligament tissue engineering.[13−15] Liu et al. and Fan et al. had demonstrated the in vitro and in vivo efficacy of silk scaffolds in the ligament tissue engineering.[14,16,17] In this study, we intend to establish a trilineage coculture system involving bone marrow mesenchymal stem cells (BMSCs) cocultured simultaneously in between ligament fibroblasts and bone osteoblasts on hybrid silk scaffolds. The BMSCs cocultured with ligament fibroblasts on one end and bone osteoblasts on the other end may be influenced by the coculture system and differentiated into fibrocartilage. We aim to evaluate the fibrocartilaginous differentiation of BMSCs and the role of cell interactions in this coculture system. The trilineage coculture system was established on hybrid silk scaffolds comprising of knitted silk embedded in silk sponge. The section of the scaffold used for seeding of osteoblasts was coated with hydroxyapatite to promote bone growth. Hydroxyapatite (HA), which is a kind of calcium phosphate mineral, is structurally similar to the natural mineral component of bone extracellular matrix (ECM). HA is believed to have biocompatibility and osteoconductivity and, thus, has been fabricated by incorporating into scaffolds in previous studies.[18−20]

Several groups have also studied the function of growth factors in the regeneration of enthesis. Previous studies focused mainly on the roles of bone morphogenetic protein (BMP) in the regeneration of the interface using different methods, such as gene delivery, directly injecting, and sustained release by means of microspheres.[21−23] Some studies also investigated the possible application of transforming growth factor (TGF) in the tendon/ligament-to-bone healing.[24−26] The transforming growth factor beta (TGF-β) family has been found to be associated with scar and adhesion formation. TGF-β1 and TGF-β3 are important modulators of musculoskeletal growth and differentiation of all the three isoforms of TGF-β in mammals.[27,28] Previous studies showed high levels of TGF-β3 isoform expressed at the tendon insertion site during early fetal development, while TGF-β1 predominated during late fetal development.[26] However, discrepancies existed and thus more studies need to be done to investigate the possible role of TGF and its isoforms in the soft tissue-to-bone healing. The role of TGF-β3 in the regeneration of ligament−bone interface was also investigated in this study using this 3D trilineage coculture model.

MATERIALS AND METHODS

Fabrication of Hybrid Silk Scaffold. Knitted scaffolds of 2 × 4 cm dimension were fabricated using raw silk fibers (*Bombyx mori*) with 14 needles on a knitting machine (Silver-reed SK270, Suzhou, China). The knitted scaffolds were degummed to remove the sericin coating from the silk fibroins, in a solution of 0.25% (w/v) Na_2CO_3 and 0.25% (w/v) sodium dodecyl sulfate (SDS) between 98 and 100 °C for 90 min, with the solution being refreshed after 45 min. The degummed silk scaffolds were then rinsed with distilled water for 1 h to remove any residual degumming solution and then air-dried. A silk fibroin solution was prepared by similarly degumming raw silk fibers and dissolving the degummed silk in a ternary solvent system of $CaCl_2$/CH_3CH_2OH/H_2O (1:2:8 molar ratio) at 69 °C with continuous stirring. The resulting silk solution was dialyzed (using a Pierce SnakeSkin pleated dialysis tubing with 10 kDa molecular weight) against distilled water for a period of 48 h. The concentration (w/v) of the dialyzed solution was determined by measuring the weight of silk fibroin obtained by freeze-drying a known volume of silk solution. The degummed knitted silk scaffold was immersed in a 2% w/v silk solution (prepared by diluting the dialyzed solution in distilled water) and freeze-dried for 24 h (using a Christ Epsilon 1−4 freeze-dryer) to allow formation of microporous silk sponges. The sponge-coated hybrid scaffolds were treated with 90/10 (v/v) methanol/water solution for 10 min to induce an amorphous to silk II conformational change in the microporous sponges to prevent resolubilization in the cell culture medium. Finally, the hybrid scaffolds were dried overnight in a fume hood.

Hydroxyapatite Coating on Hybrid Silk Scaffold. The section for the silk scaffold for osteoblasts was deposited with hydroxyapatite using an alternate soaking technology.[29] Briefly, the silk scaffold was immersed in 200 mM calcium chloride ($CaCl_2$) solution in a Petri dish placed on a mechanical shaker (150 rpm) at 37 °C for 1 h. The scaffold was then blotted on a filter paper to remove excess moisture and then immersed in a 120 mM disodium hydrogen phosphate (Na_2HPO_4) solution under the same conditions for 1 h. The alternate soaking process was repeated for three cycles. After soaking, the HA-coated silk scaffolds were washed in distilled water and air-dried at room temperature for 24 h.

Morphology Observation of the Scaffold. Morphology of hybrid silk scaffold was observed by phase contrast microscopy (Olympus IX71, Japan). Hybrid silk scaffold was coated with gold using a sputter coater (BAL-TEC Inc., CA, U.S.A.) and observed by a scanning electron microscopy (SEM, JEOL JSM-5600LV, Japan) operated at a voltage of 10 kV.

HA-coated scaffold after three cycles of HA coating using alternate soaking technology was also examined. HA-coated scaffold was freeze-dried to remove water absolutely followed by gold coating and SEM examination. HA coating on hybrid silk scaffold was also examined by Micro-CT scanner (SMX-100CT X-ray CT Sys, Shimadzu, Japan) at a X-ray voltage of 50 kV and current of 48 μA. The scans were then reconstructed to create a 3D geometry of the scaffold using VGStudioMax (version 1.2, Volume Graphics, Germany). 3D images were acquired from the software.

HA deposition on the hybrid silk scaffold was further demonstrated by Fourier transform infrared spectroscopy (FTIR). HA-coated scaffold and uncoated hybrid silk scaffold were crushed individually using a mortar and pestle. Porous sponge along with HA deposited was crushed into powder under load. The powder was pelleted in KBr and analyzed using a FTIR spectroscope (Varian FT-IR 3100, Varian, CA, U.S.A.).

Cell Isolation and Culturing. BMSCs, ligament, and bone cells were harvested from New Zealand White Rabbits (average weight, 2.5 kg) under approval of the NUS Institutional Animal Care and Use Committee, National University of Singapore. BMSCs were isolated from bone marrow aspirates according to procedures described previously.[30] Bone marrow aspirates were mixed with complete culture medium comprising Dulbecco's modified Eagle's medium with low glucose (DMEM; Gibco, Invitrogen, CA, U.S.A.), supplemented with 15% fetal bovine serum (FBS; HyClone, Logan, UT, U.S.A.) and 1% antibiotics (200 units/mL penicillin G and 200 units/mL streptomycin sulfate), and cultured at 37 °C in an incubator with 5% humidified CO_2. The cultures were replenished with fresh medium every 3−4 days. BMSCs were isolated by selective adherence to tissue culture polystyrene and nonadherent cells were removed during media change and subculturing. Semiconfluent cells of second passage (P2) were used for seeding scaffolds.

The primary ligament cells (fibroblasts) and bone cells (osteoblasts) were collected and cultured. Briefly stated, the medial collateral ligaments (MCL) of both joints and upper part of tibia were surgically removed from rabbits under anesthesia and collected in high glucose DMEM medium (HyClone, Logan, UT) with 10% FBS. MCL tissue was cut into 1 × 1 mm slices and digested with 5 mL of 0.15% collagenase-I in 37 °C shaking bath for 6 h. The bone tissue collected from femur was also cut into 2 × 2 mm pieces and digested with 5 mL of solution containing collagenase I and II (0.15% each). The semidigested ligaments and bone pieces were cultured in 60 mm Petri

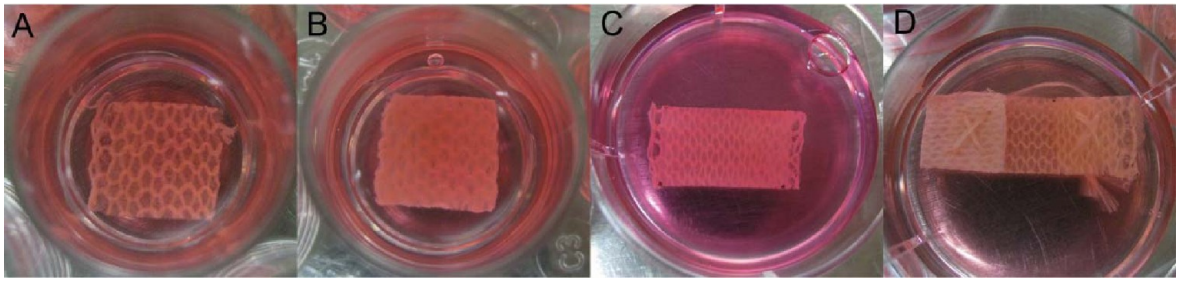

Figure 1. Images showing silk scaffolds seeded with fibroblasts (A), osteoblasts (B, HA-coated), and BMSCs (C). The scaffolds in (A–C) were cultured for 1 week and sutured together as shown in (D).

dishes with high glucose DMEM containing 10% FBS and 1% antibiotics under humidified conditions at 37 °C and 5% CO_2.

Establish a Coculture System on Silk Scaffolds. BMSCs, fibroblasts, and osteoblasts were trypsinized and seeded on the hybrid silk scaffold. Fibroblasts and osteoblasts were seeded on the silk scaffold with the dimension of 1 × 1 cm at a density of 1 × 10^5 cells/scaffold (Figure 1A,B). The section of scaffold for osteoblasts was coated with hydroxyapatite (Figure 1B). BMSCs were seeded on the silk scaffold with the dimension of 1.5 × 1 cm at a density of 2 × 10^5 cells/scaffold (Figure 1C). The three kinds of cell-seeded scaffolds were cultured separately for 1 week. After that, the scaffolds were stitched together with fibroblasts-seeded scaffold (Fb) and osteoblasts-seeded scaffold (Ob) at the two ends of BMSCs-seeded scaffold (BM; Figure 1D). The overlapped region of BMSCs-seeded scaffold with fibroblasts/osteoblasts-seeded scaffold has a dimension of about 1 × 0.5 cm. The assembled scaffolds were cultured with 10% DMEM medium (Co group) and same medium supplemented with 10 ng/mL TGF-β3 (TGF group) for another three weeks. Meanwhile, monocultured cell-seeded scaffolds (Fb, Ob, and BM) were cultured as control in 10% DMEM medium for same time.

Biochemical Study of the Coculture System. Cell viability and metabolism of the coculture system were studied after 24 h, 1, 2, and 3 weeks post seeding using the Alamar Blue colorimetric assay (Sigma, U.S.A.). The cocultured scaffolds (n = 5/group) were incubated in 5 mL of HG-DMEM supplemented with 5% FBS and 10% (v/v) Alamar Blue dye for 3 h. The absorbance of the culture media at 570/600 nm was measured in triplicates using a 96 well plate microplate reader. Using culture medium supplemented with 10% Alamar Blue dye as a reagent blank, the percentage of Alamar Blue reduction was calculated according to the formula provided by the vendor.

The total soluble glycosaminoglycan (GAG) synthesized and secreted into the culture medium by the cocultured scaffolds during the culturing period was determined. The culture medium were totally changed on days 4, 11, 18, and collected on days 7, 14, and 21. The sGAG in the medium were measured using Blyscan Assay for soluble sulfated GAG (Biocolor, Newtownabbey, Northern Ireland). According to the protocol provided by the vendor, the absorbance was measured at 656 nm, with 550 nm as the reference wavelength. A calibration curve using the GAG standard supplied by the kit was obtained, and the total amounts of sGAG were calculated using the curve.

Cell Morphology Observation by SEM. The cell morphology of monocultured BMSCs and cocultured BMSCs were observed by the JEOL JSM-5600LV (Japan) scanning electron microscopy (SEM). After coculture for three weeks, BMSCs-seeded scaffold was separated with fibroblast-seeded scaffold and osteoblast-seeded scaffold and washed with PBS. Monocultured BMSCs scaffold cultured for same time was also washed with PBS. Both of the scaffolds were then fixed in formaldehyde for 24 h and freezing dried for SEM examination. The dried scaffolds were coated with gold using a Sputter Coater (BAL-TEC Inc.) for 60 s at a current of 30 mA. Their morphology was observed with SEM operated at a voltage of 10 kV.

Quantitative RT-PCR Analysis of the Gene Expression. After cocultured for three weeks, gene expression analysis was performed to investigate the effects of coculture to the different kinds of cells in the coculture system in the gene level. The three sections of the scaffold were disassembled carefully. Monocultured fibroblasts/osteoblasts-seeded scaffold and cocultured fibroblasts/osteoblasts-seeded scaffold were labeled as mo-Fb/mo-Ob and co-Fb/co-Ob, respectively. Monocultured BMSCs-seeded scaffold was labeled as mo-BM. The cocultured BMSC-seeded scaffold was cut into three pieces (Figure 2).

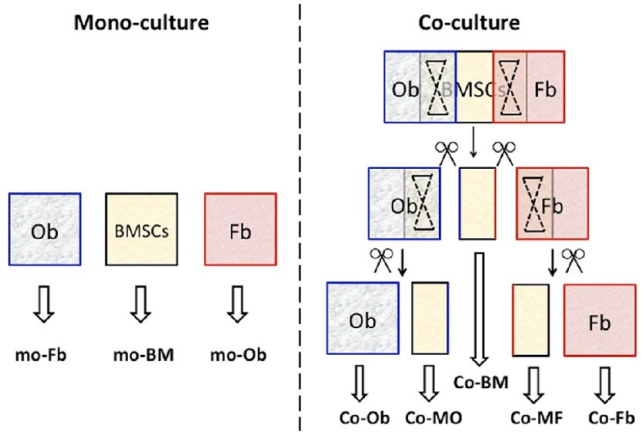

Figure 2. Schematic showing the monocultured BMSCs (mo-BM), fibroblasts (mo-Fb), and osteoblasts (mo-Ob), and cocultured BMSCs (co-MF, co-BM, and co-MO), fibroblasts (co-Fb), and osteoblasts (co-Ob) used for gene expression analysis.

The BMSC-seeded scaffold portion that was stitched to the fibroblast-seeded scaffold was labeled as co-MF. The BMSC-seeded scaffold portion that was stitched to the osteoblast-seeded scaffold was labeled as co-MO. The middle portion of BMSCs scaffold with no direct interaction with other scaffolds was labeled as co-BM. co-BM was first separated by cutting along the edges of cocultured fibroblasts and the osteoblast-seeded scaffold. The silk sutures were removed carefully. co-MO and co-MF were then separated with co-Ob and co-Fb (Figure 2). The TGF group was treated and labeled using the same basis. The BMSCs scaffolds were labeled as co-TMF, co-TMO, and co-TBM, accordingly. The cocultured fibroblasts and osteoblasts scaffolds were labeled as co-TFb and co-TOb. Total RNA was extracted from each pieces of scaffold described as above (n = 3) using Qiagen RNeasy Kit (Qiagen, Valencia, CA, U.S.A.). After that, the purity and concentration of RNA was determined by UV-spectrophotometry (S2100 Diode Array Spectrophotometer, Biochrom, Cambridge, CB, U.S.A.). cDNA synthesis was carried out using 80 ng of total RNA and reverse transcriptase (iScript, Bio-Rad Laboratories, CA, U.S.A.) with oligo (dT) primers.

Quantitative reverse transcriptase-mediated-PCR (Q-RT-PCR) was performed using SYBR-Green chemistry (iQ SYBR Green Supermix, Bio-Rad) in an iCycler iQ detection system (Bio-Rad), with glyceraldehyde three-phosphate dehydrogenase (GAPDH) as reference genes. Gene expression of different gene markers was analyzed. Fibroblasts gene markers involved collagen-type I (Col I) and tenascin-C. Osteoblasts gene markers involved Runt-related tran-

scription factor 2 (runx2) and osteonectin (ON). Fibrocartilage gene markers involved collagen-type II (Col II), sox9, and aggrecan. The primer sequences of selected genes for real-time PCR were obtained from published literature[31] (Table 1). The amplification was performed in triplicates, data were analyzed for relative expression using the ΔΔCT method, and the results were normalized to GAPDH gene expression levels.

Table 1. Primer Sequences for the Real Time RT-PCR

primer	sequences
GAPDH	F: GAC ATC AAG AAG GTG GTG AAG C
	R: CTT CAC AAA GTG GTC ATT GAG G
collagen I	F: GCA TGT CTG GTT AGG AGA AAC C
	R: ATG TAT GCA ATG CTG TTC TTG C
tenascin-C	F: TCT CTG CAC ATA GTG AAA AAC AAT ACC
	R: TCA AGG CAG TGG TGT CTG TGA
runx2	F: CCT TCC ACT CTC AGT AAG AAG A
	R: TAA GTA AAG GTG GCT GGA TAG T
osteonectin (ON)	F: GAA GTT GAG GAA ACC GAA GA
	R: GGC AGG AGG AGT CGA AG
collagen II	F: AAG AGC GGT GAC TAC TGG ATA G
	R: TGC TGT CTC CAT AGC TGA AGT
sox9	F: CTT CAT GAA GAT GAC CGA CGA G
	R: CTC TTC GCT CTC CTT CTT GAG G
aggrecan	F: GAC TGT CAG GTA CCC CAT CC
	R: CGA CGT TGC GTA AAA GAC C

Histological Sample Preparation for BMSCs Differentiation Assessments. To further characterize the differentiation of cocultured BMSCs, BMSC-seeded scaffold in the coculture system was separated after 3 weeks of culture and prepared for histological analysis. Briefly, cocultured BMSC-seeded scaffold (1 × 1.5 cm) was separated with fibroblast- and osteoblast- seeded scaffold by cutting the silk suture. Cocultured BMSC-seeded scaffold was rolled up along the long-edge of the scaffold. The rolling started from BMSC-seeded scaffold that interacted with osteoblasts-seeded scaffold (co-MO), generating a cylindrical graft with co-MO in the center and co-MF in the periphery (Figure 3). The rolled scaffold was fixed with 3.7% formaldehyde, dehydrated in 50, 70, 90, and 100% sequentially and embedded in paraffin block. The transverse cross sections were cut and histological assessments were performed.

Histological and Immunohistochemistry Staining. The paraffin-embedded cocultured BMSC sample was then sectioned and stained with hematoxylin and eosin (HE) staining for histological observation using standard protocol. Alcian Blue staining (Sigma, U.S.A.) was performed to evaluate GAG production in the extracellular matrix of BMSC scaffold according to manufacturer's protocol. Briefly, the slides were dehydrated in ethanol and stained with Alcian blue for 30 min. After rinsing in distilled water, the slides were stained with nuclear fast for 10 min. The slides were then washed and dehydrated before mounting for observation. Alizarin red S (Amresco, U.S.A.) staining was performed to evaluate the calcium deposition. The dehydrated slides were stained with Alizarin red for 5 min and dehydrated in acetone. The slides were then cleared in xylene and mounted for microscopy observation.

Immunohistochemistry staining for collagen type I (Col I), collagen type II (Col II), and aggrecan was also performed with a labeled streptavidin–biotin immunoenzymatic antigen detection system (UltraVision Detection System Anti-Mouse, HRP/DAB; LabVision, U.S.A.). According to the protocol, the sections were applied with blocking solution to block endogenous peroxidase and then digested with pepsin. The sections were then incubated with a mouse antitype I and II collagen monoclonal antibody (Sigma, U.S.A.) or a mouse antiaggrecan monoclonal antibody (Thermo, U.S.A.) before biotinylated goat anti-mouse secondary antibody and streptavidin peroxidase. DAB substrate was then added onto slides. The sections were then counterstained with hematoxylin. After dehydrating in 70, 90, and 100% ethanol and clearing in xylene, the slides were mounted with mount medium and observed by microscopy.

Statistical Analysis. All data was expressed as mean ± standard deviation (SD). All statistical analysis was performed by pairwise comparison of experimental categories using two-tailed, unpaired student *t* tests, and multiple comparisons using single-factor ANOVA and posthoc Tukey tests, using SPSS Statistics 17.0 statistical software package. A p value <0.05 was considered as statistically significant.

RESULTS

Morphology Observation of the Scaffold. Phase contrast microscopy (Figure 4A) and SEM (Figure 4B)

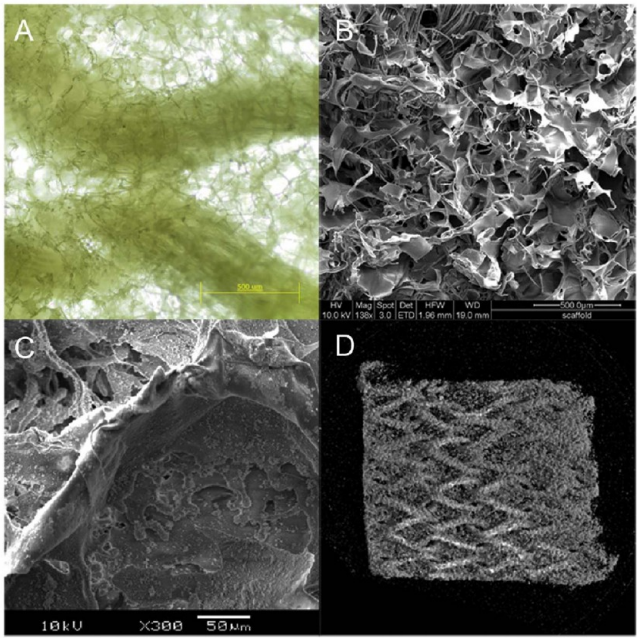

Figure 4. Morphology observation of the hybrid silk scaffold by phase contrast microscopy (A) and SEM (B). HA-coated silk scaffold for three soaking cycles was observed by SEM (C) and micro-CT (D).

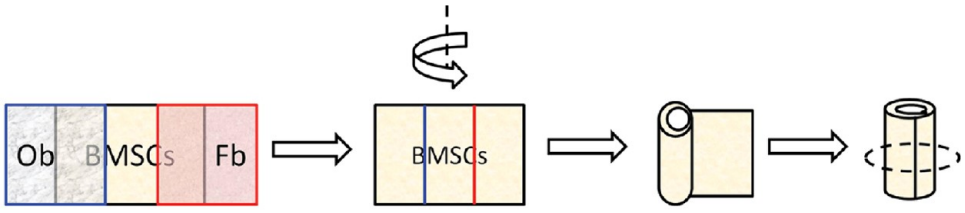

Figure 3. Schematic showing cocultured BMSC-seeded scaffold was separated from fibroblast- and osteoblast-seeded scaffolds in the cocultured system. The isolated BMSC-seeded scaffold was rolled up along its long edge to form a cylindrical structure and then processed for histological analysis. The histological sections were cut to reveal the transverse cross section of the cylindrical structure.

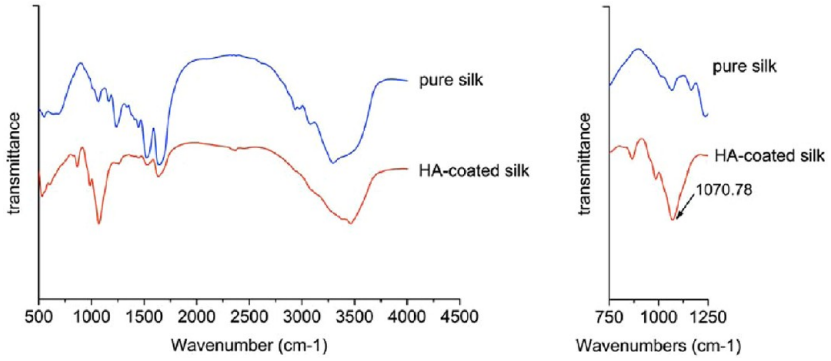

Figure 5. FTIR spectra of hybrid silk scaffold and HA-coated silk scaffold. A characteristic peak of PO_4^{3-} was found at 1070.78 in the HA-coated silk scaffold, as indicated by the arrow.

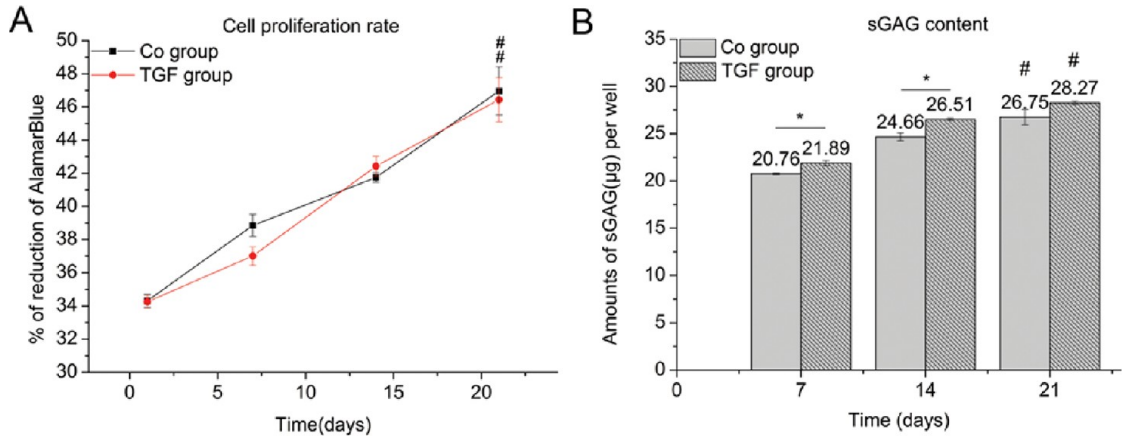

Figure 6. Cell proliferation rate (A) and total soluble GAG amounts (B) of the trilineage coculture system without (Co group) and with TGF-β3 supplementation (TGF group) during a 3 week culturing period (*p < 0.05, t test; #p < 0.05, ANOVA).

demonstrated an interconnected microporous silk sponge formed in the pores and spreading over the surface of the knitted silk scaffold. The pore sizes of the silk sponge ranged from 80 to 250 μm. The average pore size of the hybrid silk scaffold was 154.5 ± 54.6 μm. Nanoscale HA particles were successfully deposited and distributed on the surface of silk sponge, as observed by SEM (Figure 4C). Micro-CT observation also demonstrated the calcium deposition on hybrid silk scaffold (Figure 4D). HA deposition was further demonstrated by FTIR spectroscopy. Compared with uncoated hybrid silk scaffold, the FTIR spectra of the HA-coated silk scaffolds showed a peak at 1070.78, corresponding to the characteristic peak of phosphate groups of hydroxyapatite (Figure 5).

Biochemical Study of the Coculture System. The cell viability/proliferation of the cocultured scaffolds in the Co and TGF groups was assessed using the Alamar Blue assay (Figure 6A). At each time point, the cell proliferation of both groups showed significant increases (*p < 0.05). However, there was no significant difference in cell proliferation between these two groups.

Soluble glycosaminoglycan secreted into medium by the cocultured groups was evaluated (Figure 6B). Both groups showed significant increases in soluble GAGs with the increase in culturing time (#p < 0.05). In the Co group, the amount of sGAGs increased from 20.8 ± 0.2 μg/well on day 7 to 24.7 ± 0.7 μg/well on day 14 and 26.8 ± 1.4 μg/well on day 21. In the TGF group, amounts of sGAGs increased from 21.9 ± 0.5 μg/well on day 7 to 26.5 ± 0.2 μg/well on day 14 and 28.3 ± 0.3 μg/well on day 21. On both day 7 and day 14, the TGF group showed a significantly larger amount of secreted sGAGs than the Co group (*p < 0.05). No significant difference was found in the two groups on day 21.

Gene Expression Analyses. Expression of fibroblast gene markers and osteoblast gene markers were analyzed to evaluate the effects of the coculture system on the gene expression of mature cells (fibroblasts and osteoblasts). Compared to monocultured mature fibroblasts (mo-Fb) and osteoblasts (mo-Ob), cocultured fibroblasts (co-Fb) and osteoblasts (co-Ob) maintained their properties in gene level (Figure 7A,C). co-Fb had an upregulation of collagen 1 and a downregulation of tenascin-C with respect to mono-Fb. However, there was no significant difference in the gene expression between co-Fb and mono-Fb. co-Ob showed up-regulation of both runx2 and osteonectin. It was also found cocultured BMSCs scaffolds that interacted with osteoblasts (co-MO) also expressed osteoblasts gene markers runx2 and osteonectin. However, the cocultured BMSC scaffold that interacted with fibroblasts (co-MF) did not show an equivalent expression of tenascin-C compared to mo-Fb (significant down-regulation in co-MF). In the TGF-treated group, both co-TFb and co-TOb showed significant up-regulation of gene expression compared with mo-Fb and mo-Ob, respectively (Figure 7B,D). This was also observed in co-TMO and co-TMF in the TGF group, which showed up-regulated fibroblasts gene markers. The supplementation of

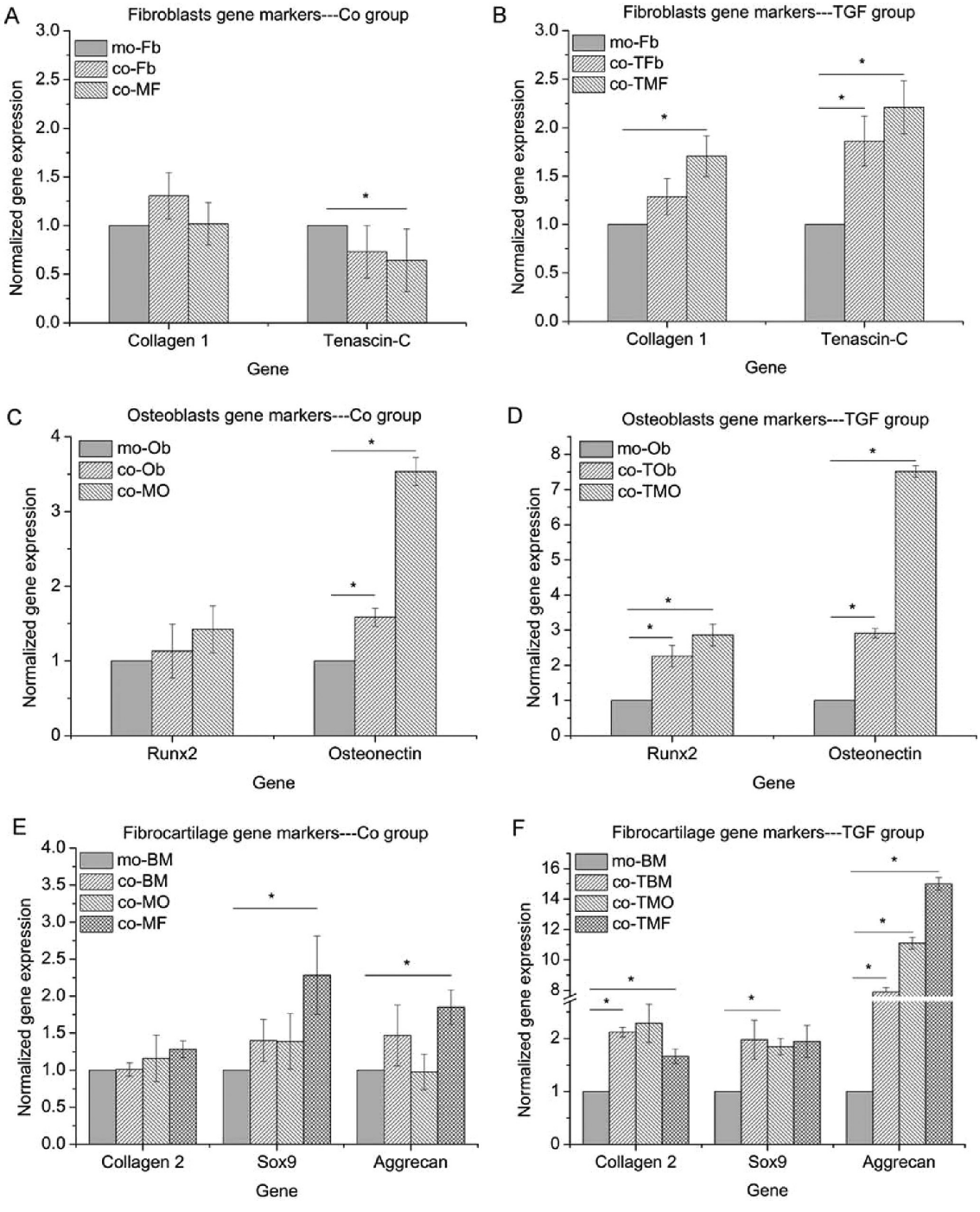

Figure 7. Gene expression analysis of fibroblasts gene markers (A, B), osteoblasts gene markers (C, D), and fibrocartilage gene markers (E, F) after three weeks of culture (*$p < 0.05$, t test).

TGF enhanced the specific gene markers expression in coculture mature fibroblasts and osteoblasts.

Expression of fibrocartilage gene markers was analyzed to evaluate the potential of BMSCs' differentiation into intermediate fibrocartilage. When compared against monocultured BMSCs, cocultured BMSCs scaffold (co-MO, co-BM, and co-MF) showed up-regulation of fibrocartilage gene markers (Figure 7E). This effect was enhanced following the addition of TGF into the coculture system (Figure 7F). Combined with the fibroblasts and osteoblasts gene marker expressions in co-MO and co-MF, these results may indicate the differentiation of BMSCs into an osteochondrogenic lineage instead of a fibroblastic lineage.

Cell Morphology Observation by SEM. The cell morphology showed phenotype alteration of BMSCs cultured in the coculture system compared with monocultured BMSCs (Figure 8). Monocultured BMSCs were found to attach onto the silk sponge of the scaffold and had a more spread-out phenotype. The cells were connected to adjacent cells and formed a fibrous network. However, cocultured BMSCs showed a rounded phenotype, the beads-like cells were distributed in the cell network and wrapped by secreted extracellular matrix (ECM). The phenotype of cocultured

dx.doi.org/10.1021/bm300651q | Biomacromolecules 2012, 13, 2692−2703

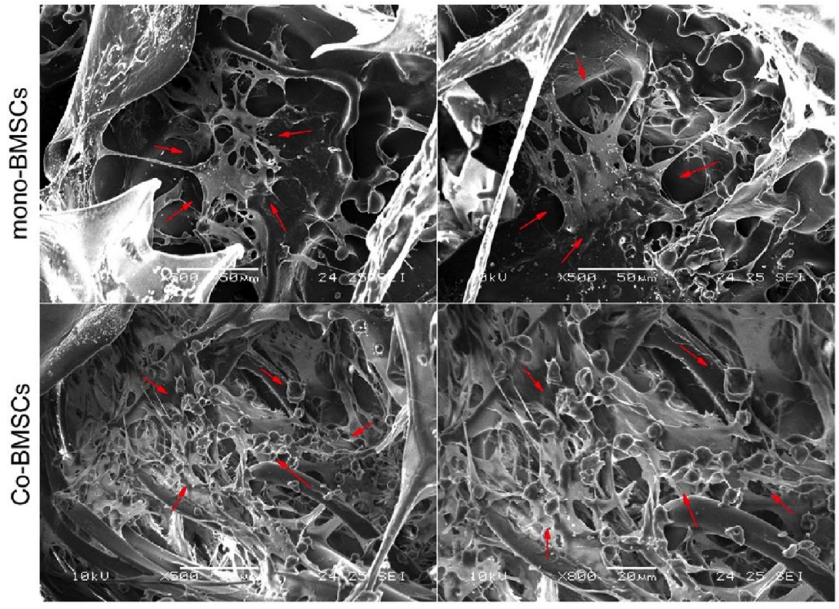

Figure 8. SEM observation of cell morphology of monocultured BMSCs (mo-BM) and cocultured BMSCs (co-BM) on the silk scaffold after culturing for three weeks. Attached cells on the scaffold were labeled using red arrows.

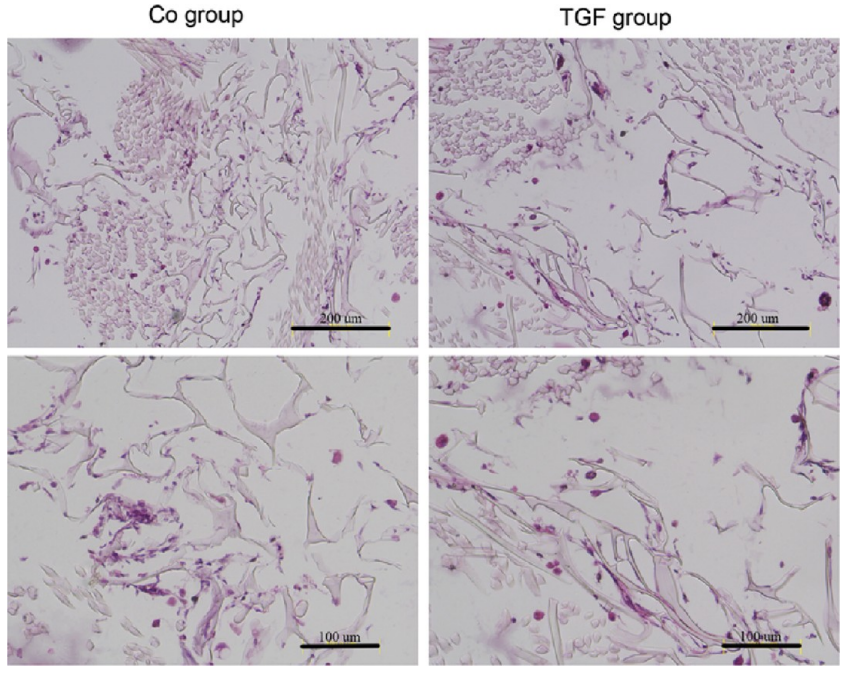

Figure 9. H&E staining observation of cocultured BMSCs on the silk scaffold in Co and TGF groups after culturing for three weeks.

BMSCs observed was similar to the phenotype of cells of osteochondral lineage.

Histology and Immunohistochemistry Study. The cross-sectional view of cell distribution in the hybrid silk scaffold was observed by H&E staining (Figure 9). Cells were distributed in the sponge and even deep into the core of knitted silk, which also demonstrated that the porous scaffold was interconnected and allowed the cells to penetrate the entire scaffold. No significant difference in cell amounts was observed between the Co and TGF groups from H&E staining.

GAG deposition in the ECM of BMSCs in the cocultured BMSCs-seeded scaffold was demonstrated by Alcian blue staining. GAGs were distributed extensively throughout the cocultured BMSCs scaffold both in the Co group and in the TGF group (Figure 10). GAG distribution could be observed in the silk sponge and knitted silk scaffolds in both of the two groups. However, the Co and TGF groups showed different results in calcium deposition, which was demonstrated by Alizarin Red S staining (Figure 11). In the Co group, calcium deposition indicated by red staining was found in the center of the scaffolds, where the co-MO was located. No calcium deposition was found in co-MF region. In the TGF groups, no calcium was deposited in both co-MO and co-MF regions.

Immunohistochemistry studies further confirmed the differentiation of BMSCs in the coculture system (Figure 12). Positive staining for collagen I, collagen II, and aggrecan were

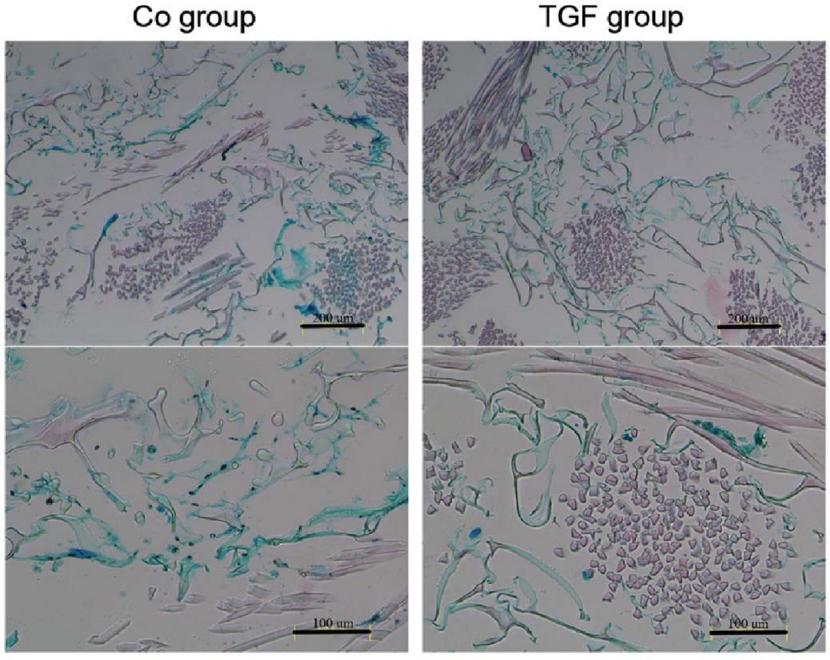

Figure 10. Alcian blue staining observation for GAG distribution of cocultured BMSCs on the silk scaffold in Co and TGF groups after culturing for three weeks.

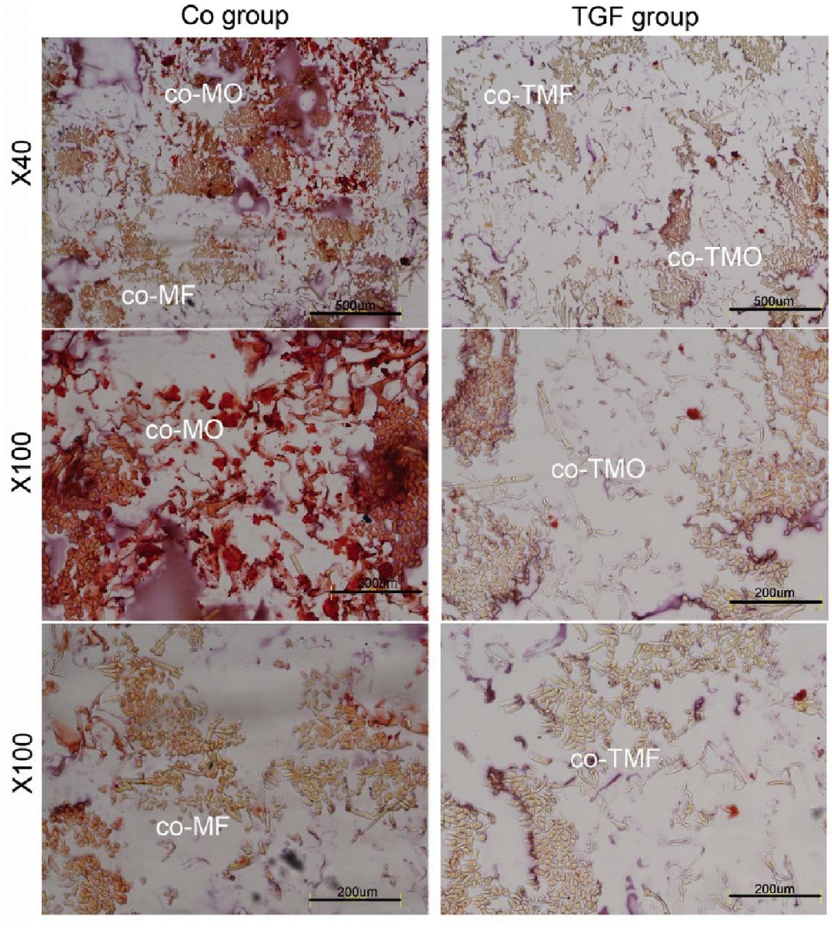

Figure 11. Alizarin red S staining observation for calcium deposition of cocultured BMSCs on the silk scaffold in Co group and TGF group for three weeks. co-MO/co-TMO: cocultured BMSCs-seeded scaffold stitched with osteoblasts-seeded scaffold in Co and TGF groups. co-MF/co-TMF: cocultured BMSC-seeded scaffold sutured with fibroblast-seeded scaffold in Co and TGF groups.

dx.doi.org/10.1021/bm300651q | *Biomacromolecules* 2012, 13, 2692−2703

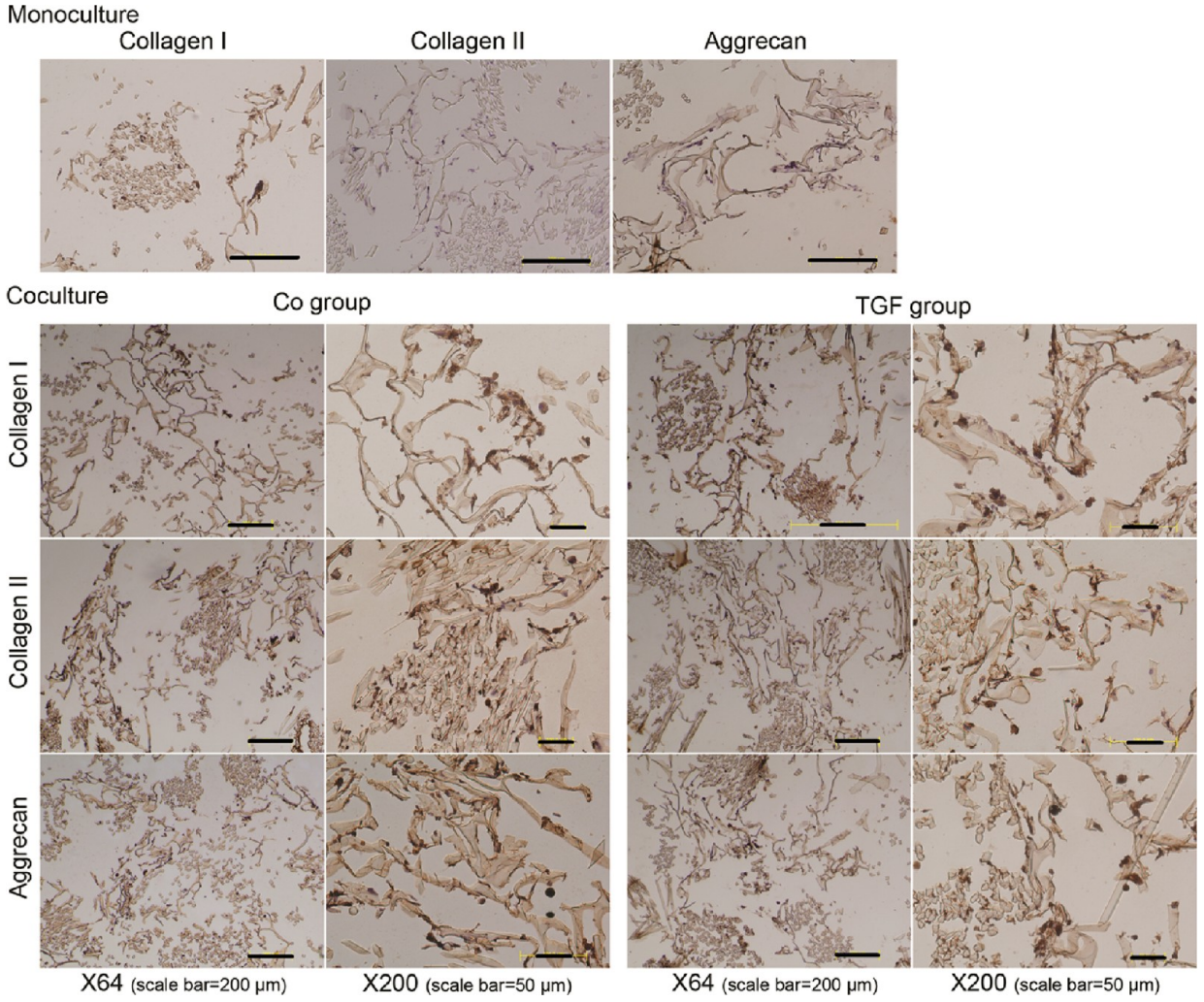

Figure 12. Immunohistochemistry staining of collagen I, collagen II, and aggrecan in the ECM of cocultured BMSCs on the silk scaffold in the Co and TGF groups after culturing for three weeks. Monoculture: monocultured BMSC-seeded silk scaffold (scale bar = 100 μm). Coculture: cocultured BMSC-seeded silk scaffold in the Co and TGF groups.

found in both Co and TGF groups. Monocultured BMSCs also showed positive staining of collagen I, which was indicated by a brown color. Blue cell nuclei stained by hemotoxylin could be observed in collagen II and aggrecan-stained monocultured BMSCs, and no brown color was observed. Compared with monoculture, in the Co and TGF group, cell nuclei were wrapped by a brown color-stained matrix, which demonstrated the existence of collagen II and aggrecan. These results are consistent with those obtained from RT-PCR.

■ DISCUSSION

This study managed to establish a trilineage cocultured system (osteoblasts−BMSCs−fibroblasts) on hybrid silk scaffolds, and the influence of the coculture system on the undifferentiated BMSCs was successfully investigated. Cell-to-cell interaction may play an important role in the regeneration of enthesis which is a multiphasic structure that involves bone, ligament (or tendon) and fibrocartilaginous intermediate stage.[6,11] Our study demonstrated that BMSCs cultured between osteoblasts and fibroblasts in the 3D cell coculture system on the hybrid silk scaffold were able to differentiate toward the fibrocartilage lineage.

Recently, a coculture system has been used as an approach that can provide efficient cell−cell interactions to better mimic the native environment of the tissue.[32] For the coculture system, previous studies have shown that when differentiated mature cells are cocultured with differentiated cells, cells maintain their specific cell phenotype and cell metabolism is often influenced by the coculture system. However, cell differentiation would occur when undifferentiated stem cells were cocultured with differentiated mature cells.[33,34] In our study, based on the real time RT-PCT results, cocultured osteoblasts and fibroblasts were found to maintain their cell lineage phenotype. However, cocultured BMSCs were found to differentiate toward the fibrocartilage lineage. The cocultured BMSCs on the hybrid silk scaffold showed an upregulation of fibrocartilage interface-relevant gene markers, collagen II, sox9, and aggrecan when compared to monocultured BMSCs (Figure 7E). Histological staining and immunohistochemistry analysis further confirmed the results. Positive immunohistochemistry staining of collagen II, sox9, and aggrecan was found (Figure 12). Aggrecan has been found to be prominent in the enthesis by immunohistochemistry labeling.[35] Glycosaminoglycans (GAGs) are also typical components of the ECM at enthesis.[36] The presence of GAG in the ECM was confirmed by Alcian

dx.doi.org/10.1021/bm300651q | *Biomacromolecules* 2012, 13, 2692−2703

blue staining in our study (Figure 10). These results demonstrated that differentiation of BMSCs had taken place in the trilineage coculture system. SEM observation of cocultured BMSCs showed changes in cell morphology, which might be due to cell differentiation (Figure 8). Monocultured BMSCs showed a flat and stretched-out morphology on the surface of the hybrid silk scaffold. However, cocultured BMSCs were observed to present a beads-like spherical morphology with ECM wrapped around spherical cells, which is similar to cell morphology of osteochondral lineage.

In our study, the trilineage coculture system was applied onto hybrid silk scaffolds. The knitted silk provided mechanical support, while the microporous silk sponge facilitated cell attachment and proliferation in the hybrid system, and BMSC-seeded scaffolds showed good biocompatibility and improved biomechanical properties of ligament repair in rabbit and pig models.[16,17] The scaffold constructed in this study has pore sizes ranging from 80 to 250 μm. It is reported that a pore size diameter of 200−250 μm is suitable for ligaments regeneration, while pore sizes need to be greater than 100 μm for bone ingrowth.[37,38] The microsponge structure is interconnected and the pore size diameter partially overlaps with the optimal pore size previously reported. These properties would enable the hybrid silk scaffolds to provide the appropriate environment for the proliferation and interaction of the seeded cells. This support of the silk scaffold could be demonstrated by increased cell proliferation during the culture period (Figure 6A). SEM also showed the scaffold supported the cell attachment and differentiation (Figure 8). The scaffold could be fabricated by coating hydroxyapatite regionally to create a suitable phase for bone growth, thus forming a multisegmental scaffold for the trilineage coculture of osteoblasts−BMSCs−fibroblasts. This study investigated influences of the trilineage coculture system using scaffolds that were stitched together, which had distinct regions to study the roles of osteoblasts and fibroblasts in the differentiation of BMSCs. In this structure, differences were found in the differentiation of BMSCs that interacted with osteoblasts and fibroblasts. co-MO (BMSCs interacting with osteoblasts) showed an up-regulated expression of osteoblast-relevant gene markers runx2 and ON (Figure 7C), while co-MF (BMSCs interacting with fibroblasts) showed a down-regulated expression of fibroblast-relevant gene markers tenascin-C (Figure 7A). On the other hand, co-MF showed significant up-regulation of sox9 expression than co-MO, which is an early gene marker expressed in chondrogenic differentiation. Although immunohistochemistry staining for fibrocartilage-relevant gene markers showed differentiation of co-MO and co-MF into fibrocartilage lineage, it seems that they belong to different stages of differentiation of BMSCs. Alizarin Red S staining for calcium confirmed the findings (Figure 11). The results showed calcium deposition in co-MO, while no calcium deposition was found in co-MF. This may indicate a gradual transition in the BMSC-seeded intermediate region from uncalcified fibrocartilage to calcified fibrocartilage. This may be due to co-MO directly interacting with a HA-coated osteoblast-seeded silk scaffold. Besides cellular influence, HA deposition on the osteoblast-seeded scaffold may also play a role in inducing the differentiation of co-MO into osteochondrogenic lineage.

The role of TGF-β3 in the regeneration of interface has been investigated in previous studies. Kim et al. found that application of TGF-β1 in rat supraspinatus tendons promoted low-quality scar tissue formation, while no significant improvement in healing with the application of TGF-β3.[24] However, Chan et al. found that TGF-β3 exhibited the highest potency in stimulating the deposition of procollagen types I and III.[25] Manning et al. reported controlled release of TGF-β3 accelerated the in vivo healing process in the rat supraspinatus tendons using a heparin/fibrin-based delivery system.[39] In our study, the role of TGF-β3 in the regeneration of interface in the 3D cocultured model has been investigated by adding TGF-β3 into the coculture system. Cells maintained their viability and increased proliferation was observed during culture period in TGF group, which was indicated by Alamar Blue assay (Figure 6). TGF-β was found to inhibit cell proliferation of many cell types such as epithelial and endothelial cells but stimulate cell proliferation of some other cell types (skin fibroblasts, mesangial cell, etc.).[40] The mechanism of how TGF-β controls cell proliferation is still under investigation. Compared with the coculture system without TGF-β3, TGF-β3 had no inhibitory or enhancing effect to cell proliferation of the whole coculture system. The supplement of TGF-β3 was found to increase the secretion of the sGAG amount compared to the untreated coculture system in the first two weeks (Figure 6B). No significant increase in sGAG amount was observed after three weeks of culture, which also could be demonstrated by Alcian blue staining after three weeks of culturing (Figure 10). The supplement of TGF-β3 showed enhanced gene expression of both mature cells and BMSCs. This may indicate that the supplementation of TGF-β3 speeded up the differentiation of cocultured BMSCs. The effects of TGF-β3 supplement to the coculture system were also observed in Alizarin Red S staining (Figure 11). No calcium deposition was found in the TGF group, which was different than the result of cocultured BMSCs in the Co group. In the RT-PCR analysis, upregulation of osteonectin was observed in co-TMO in the presence of TGF-β3. Osteonectin is an acidic calcium-binding protein and plays roles in bone mineralization, cell−matrix interaction, and collagen binding. Osteonectin could be found in osteoblasts and hypertrophic chondrocytes. Pacifici et al. found that osteonectin is synthesized by chondrocytes in each zone of growth cartilage but secreted and accumulated only in the mineralized zone.[41] TGF-β signaling has been shown to preserve adequate chondrocytes within the growth plate by inhibiting the hypertrophic differentiation and controlling matrix synthesis.[42] It may be concluded that osteonectin was synthesized but not accumulated because the hypertrophic differentiation was inhibited by the presence of TGF-β3 in our coculture system. On the other hand, several studies have shown that TGF-β3 has roles of inhibiting mineralization. Controlled release of TGF-β3 encapsulated in poly(DL-lactic-*co*-glycolic acid) (PLGA) microspheres was found to inhibit the osteogenic differentiation of hMSCs, as evidenced by significantly reduced alkaline phosphatase activity and staining, as well as decreased mineral deposition.[43] Guo et al. also found the role of TGF-β3 in delaying the mineralization process using a chondrogenic−osteogenic bilayered hydrogel composite. Rabbit BMSCs encapsulated with TGF-β3-loaded microspheres were seeded in the chondrogenic layer and cocultured with BMSCs after different periods of osteogenic preculture (0, 3, 6, and 12 days) in the osteogenic layer. They observed alkaline phosphatase activity was maintained but no calcium staining was observed.[44]

This study demonstrated the possible role of the trilineage coculture system in the differentiation of BMSCs cultured on

the hybrid silk scaffold. Silk scaffold was also shown to have the ability to provide a 3D environment for the trilineage coculture. Furthermore, the hybrid silk scaffolds possess good tensile properties and a slow degradation rate, which has advantages over other commonly used natural and synthetic materials such as collagen and PLGA. Silk scaffold constructed by Liu et al. in our group recorded a maximum tensile load of 257 ± 7 N, which is much higher than PLGA and PLLA knitted scaffold.[14] As an in vitro model, the trilineage coculture system established in this study demonstrated positive influence of ligament−bone interface relevant cells (ligament fibroblasts and bone osteoblasts) on fibrocartilage differentiation of BMSCS. Based on this study, a bone−ligament−bone graft with a native-like fibrocartilage interface can be constructed using hybrid silk scaffold and coculture system. Hybrid silk scaffold would be further fabricated with regional deposition of hydroxyapatite on the bone ends and the trilineage coculture system would be applied with the scaffold. Hydroxyapatite coating may lead to bone-to-bone healing and the native-like fibrocartilage interface may provide good graft integration. The knitted silk will function as mechanical support for the graft. Such a bone−ligament−bone graft may be more promising than current tissue engineered ligament-alone graft.

CONCLUSIONS

In our study, we developed a trilineage coculture system (osteoblasts−BMSCs−fibroblasts) on a hybrid silk scaffold by stitching three pieces of cell-seeded scaffold together. The silk scaffold contains porous sponge which is suitable for cell proliferation. Furthermore, the scaffold can be coated with hydroxyapatite to enhance osteoblasts activities. The influences of this coculture system on the differentiation of BMSCs were investigated. RT-PCR results and immunohistochemistry results demonstrated that BMSCs cultured in between fibroblasts and osteoblasts had differentiated into the fibrocartilage lineage. The morphological change caused by differentiation was also observed by SEM observation. We also found calcium deposition in the region of BMSC-seeded scaffold that was adjacent to the osteoblast-seeded scaffold, while no calcium deposition was found in the region that was adjacent to the fibroblast-seeded scaffold. Thus, a gradual transition from uncalcified to calcified region was formed in the cocultured BMSCs. This transition was not found in the cocultured scaffold supplemented with 10 ng/mL TGF-β3, although similar result of fibrocartilage differentiation of BMSCs was observed. This may indicate TGF-β3 has a delayed effect on the mineralization process of chondrocytes.

AUTHOR INFORMATION

Corresponding Author

*Tel.: +65-6516-4257. Fax: +65-6776-5322. E-mail: biegohj@nus.edu.sg.

Notes

The authors declare no competing financial interest.

ACKNOWLEDGMENTS

This study was supported by the Biomedical Research Council, Singapore, and Faculty of Engineering, National University of Singapore.

REFERENCES

(1) Griffin, L. Y.; Albohm, M. J.; Arendt, E. A.; Bahr, R.; Beynnon, B. D.; DeMaio, M.; Dick, R. W.; Engebretsen, L.; Garrett, W. E.; Hannafin, J. A.; Hewett, T. E.; Huston, L. J.; Ireland, M. L.; Johnson, R. J.; Lephart, S.; Mandelbaum, B. R.; Mann, B. J.; Marks, P. H.; Marshall, S. W.; Myklebust, G.; Noyes, F. R.; Powers, C.; Shields, C.; Shultz, S. J.; Silvers, H.; Slauterbeck, J.; Taylor, D. C.; Teitz, C. C.; Wojtys, E. M.; Yu, B. *Am. J. Sports Med.* **2006**, *34*, 1512−1532.
(2) Kurosaka, M.; Yoshiya, S.; Andrish, J. T. *Am. J. Sports Med.* **1987**, *15*, 225−229.
(3) Shaw, H. M.; Benjamin, M. *Scand. J. Med. Sci. Sports* **2007**, *17*, 303−315.
(4) Benjamin, M.; Kumai, T.; Milz, S.; Boszczyk, B. M.; Boszczyk, A. A.; Ralphs, J. R. *Comp. Biochem. Physiol., A: Mol. Integr. Physiol.* **2002**, *133*, 931−945.
(5) Benjamin, M.; Ralphs, J. R. *J. Anat.* **1998**, *193*, 481−494.
(6) Gao, J.; Messner, K.; Ralphs, J. R.; Benjamin, M. *Anat. Embryol. (Berlin)* **1996**, *194*, 399−406.
(7) Benjamin, M.; McGonagle, D. *Scand. J. Med. Sci. Sports* **2009**, *19*, 520−527.
(8) Claudepierre, P.; Voisin, M. C. *Joint Bone Spine* **2005**, *72*, 32−37.
(9) Lu, H. H.; Jiang, J. *Adv. Biochem. Eng. Biotechnol.* **2006**, *102*, 91−111.
(10) Wang, I. N. E.; Shan, J.; Choi, R.; Oh, S.; Kepler, C. K.; Chen, F. H.; Lu, H. H. *J. Orthop. Res.* **2007**, *25*, 1609−20.
(11) Spalazzi, J. P.; Dagher, E.; Doty, S. B.; Guo, X. E.; Rodeo, S. A.; Lu, H. H. *J. Biomed. Mater. Res., A* **2008**, *86A*, 1−12.
(12) Lim, J. K.; Hui, J.; Li, L.; Thambyah, A.; Goh, J.; Lee, E. H. *Arthroscopy* **2004**, *20*, 899−910.
(13) Altman, G. H.; Horan, R. L.; Lu, H. H.; Moreau, J.; Martin, I.; Richmond, J. C.; Kaplan, D. L. *Biomaterials* **2002**, *23*, 4131−4141.
(14) Liu, H. F.; Fan, H. B.; Wang, Y.; Toh, S. L.; Goh, J. C. H. *Biomaterials* **2008**, *29*, 662−674.
(15) Liao, S.; Chan, C. K.; Ramakrishna, S. *Mater. Sci. Eng., C* **2008**, *28*, 1189−1202.
(16) Fan, H. B.; Liu, H. F.; Toh, S. L.; Goh, J. C. H. *Biomaterials* **2009**, *30*, 4967−4977.
(17) Fan, H. B.; Liu, H. F.; Wong, E. J. W.; Toh, S. L.; Goh, J. C. H. *Biomaterials* **2008**, *29*, 3324−3337.
(18) Dorozhkin, S. V. *Biomaterials* **2010**, *31*, 1465−1485.
(19) LeGeros, R. Z. *Clin. Orthop. Relat. Res.* **2002**, 81−98.
(20) Swetha, M.; Sahithi, K.; Moorthi, A.; Srinivasan, N.; Ramasamy, K.; Selvamurugan, N. *Int. J. Biol. Macromol.* **2010**, *47*, 1−4.
(21) Hashimoto, Y.; Yoshida, G.; Toyoda, H.; Takaoka, K. *J. Orthop. Res.* **2007**, *25*, 1415−1424.
(22) Martinek, V.; Latterman, C.; Usas, A.; Abramowitch, S.; Woo, S. L. Y.; Fu, F. H.; Huard, J. *J. Bone Joint Surg. Am.* **2002**, *84A*, 1123−1131.
(23) Lee, J.; Il Choi, W.; Tae, G.; Kim, Y. H.; Kang, S. S.; Kim, S. E.; Kim, S. H.; Jung, Y. *Acta Biomater.* **2011**, *7*, 244−257.
(24) Kim, H. M.; Galatz, L. M.; Das, R.; Havlioglu, N.; Rothermich, S. Y.; Thomopoulos, S. *Connect Tissue Res.* **2011**, *52*, 87−98.
(25) Chan, K. M.; Fu, S. C.; Wong, Y. P.; Hui, W. C.; Cheuk, Y. C.; Wong, M. W. N. *Wound Repair Regen.* **2008**, *16*, 399−407.
(26) Galatz, L.; Rothermich, S.; VanderPloeg, K.; Petersen, B.; Sandell, L.; Thomopoulos, S. *J. Orthop. Res.* **2007**, *25*, 1621−1628.
(27) Merino, R.; Ganan, Y.; Macias, D.; Economides, A. N.; Sampath, K. T.; Hurle, J. M. *Dev. Biol.* **1998**, *200*, 35−45.
(28) Galatz, L. M.; Sandell, L. J.; Rothermich, S. Y.; Das, R.; Mastny, A.; Havlioglu, N.; Silva, M. J.; Thomopoulos, S. *J. Orthop. Res.* **2006**, *24*, 541−550.
(29) Furuzono, T.; Taguchi, T.; Kishida, A.; Akashi, M.; Tamada, Y. *J. Biomed. Mater. Res., A* **2000**, *50*, 344−352.
(30) Sahoo, S.; Ang, L. T.; Goh, J. C. H.; Toh, S. L. *Differentiation* **2010**, *79*, 102−110.
(31) See, E. Y. S.; Toh, S. L.; Goh, J. C. H. *Tissue Eng., Part A* **2010**, *16*, 1421−1431.
(32) Hendriks, J.; Riesle, J.; van Blitterswijk, C. A. *J. Tissue Eng. Regen. Med.* **2007**, *1*, 170−178.

(33) Jiang, J.; Nicoll, S. B.; Lu, H. H. *Biochem. Biophys. Res. Commun.* **2005**, *338*, 762−770.
(34) Spalazzi, J. P.; Dionisio, K. L.; Jiang, J.; Lu, H. H. *IEEE Eng. Med. Biol. Mag.* **2003**, *22*, 27−34.
(35) Benjamin, M.; Toumi, H.; Ralphs, J. R.; Bydder, G.; Best, T. M.; Milz, S. *J. Anat.* **2006**, *208*, 471−490.
(36) Milz, S.; Tischer, T.; Buettner, A.; Schieker, M.; Maier, M.; Redman, S.; Emery, P.; McGonagle, D.; Benjamin, M. *Ann. Rheum. Dis.* **2004**, *63*, 1015−1021.
(37) Laurencin, C. T.; Freeman, J. W. *Biomaterials* **2005**, *26*, 7530−7536.
(38) Gross, K. A.; Rodriguez-Lorenzo, L. M. *Biomaterials* **2004**, *25*, 4955−4962.
(39) Manning, C. N.; Kim, H. M.; Sakiyama-Elbert, S.; Galatz, L. M.; Havlioglu, N.; Thomopoulos, S. *J. Orthop. Res.* **2011**, *29*, 1099−1105.
(40) Huang, S. S.; Huang, J. S. *J. Cell. Biochem.* **2005**, *96*, 447−462.
(41) Pacifici, M.; Oshima, O.; Fisher, L. W.; Young, M. F.; Shapiro, I. M.; Leboy, P. S. *Calcif. Tissue Int.* **1990**, *47*, 51−61.
(42) Yang, X.; Chen, L.; Xu, X. L.; Li, C. L.; Huang, C. F.; Deng, C. X. *J. Cell Biol.* **2001**, *153*, 35−46.
(43) Moioli, E. K.; Hong, L.; Mao, J. J. *Wound Rep. Regen.* **2007**, *15*, 413−421.
(44) Guo, X.; Liao, J.; Park, H.; Saraf, A.; Raphael, R. M.; Tabata, Y.; Kasper, F. K.; Mikos, A. G. *Acta Biomater.* **2010**, *6*, 2920−2931.